Research Journal of Applied Sciences, Engineering and Technology 6(17): 3214-3221, 2013
DOI:10.19026/rjaset.6.3626
ISSN: 2040-7459; e-ISSN: 2040-7467

Submitted: January 15, 2013 Accepted: February 18, 2013 Published: September 20, 2013

Research Article

Modeling and Control of a Quadrotor Helicopter System under Impact of Wind Field

Yanmin Chen, Yongling He and Minfeng Zhou
School of Transportation Science and Engineering, Beihang University, Beijing, 100191, China

Abstract: Aiming at the hovering problem of a quadrotor helicopter system under impact of wind field, in this study, a nonlinear integral backtepping controller was designed. The quadrotor helicopter is a nonlinear system which is underactuated and strongly coupled. The wind field would lead to the nonlinear change of aerodynamic force and moment and make the flight condition worse. For the highly nonlinear characteristic of the system, first we establish the dynamic model that considers the effect of wind field via Newton-Euler formalism; and then we develop a controller based on integral backstepping algorithm and validate the stability of the system by Lyapunov theory. Simulation results demonstrate that the model can accurately reflects dynamic performance of the system and the controller presents good robustness in the effect of wind field.

Keywords: Attitude control, integral backstepping, lyapunov theory, position control, quadrotor helicopter, wind field

INTRODUCTION

Recently, as a member of Vertical Take-Off and Landing (VTOL) Unmanned Aerial Vehicles (UAVs), the quadrotor helicopter has been more widely used in both military and civilian fields. Compared to fixed-wing aircrafts, quadrotors can fly at low altitude and hovering at set point. Compared to traditional helicopters, quadrotors have several advantages including: simple mechanical structure, good maneuverability and small size, low cost and strong concealment. These excellent features make quadrotors able to perform in constrained area with more effectiveness and reliability.

The quadrotor system is highly nonlinear because the aerodynamic of the four rotors. Like traditional aircraft, the control of quadrotor involves attitude control and position control. The main difference is that, due to unique body structure as well as rotor aerodynamic, the attitude dynamics and position dynamics are strongly coupled (Abhijit *et al*., 2009). Moreover, because the motion of the quadrotor is six degrees of freedom (6 DOF) but with only four driving forces, so the system is underactuated.

In the relevant literatures, a lot of work has been done to deal with the problem of modeling and control of the quadrotor system. Hoffmann *et al*. (2009, 2011) developed the STARMAC || research platform to validate multiple algorithms such as reactive collision avoidance, path planning, cooperative search and aggressive maneuvering. In the early study, PID control scheme is widely used. Bouabdallah *et al*. (2004) used PID control and LQ regulation to control the system. Salih *et al*. (2010) introduced a PID controller to the set point flight of a quadrotor. Compared to linear control method, nonlinear control method can substantially enhance the capability of the controller. As a kind of nonlinear control method, backstepping control was implemented by many researches (Bouabdallah and Siegwart, 2007; Ashfaq and Wang, 2008; Bouchoucha *et al*., 2011; Madani and Benallegue, 2006a). Ashfaq and Wang (2008) proposed a backstepping-based PID controller for a quadrotor under the condition of hovering and near hovering. Bouchoucha *et al*. (2011) developed an integral backstepping controller for attitude tracking. Madani and Benallegue (2006b) presented a full-state backstepping technique based on Lyapunov stability theory. There are also other nonlinear control methods used for the control of quadrotor system. Raffo *et al*. (2010) presented an integral predictive and nonlinear robust control strategy to solve the path following problem. Lee *et al*. (2009) discussed the effect of feedback linearization controller and sliding mode controller for trajectory tracking control. Carrillo *et al*. (2011) proposed a vision-based position control method; this method can measure the position variables that are difficult to compute when using conventional navigation systems.

However, few researches considered the impact of wind field on modeling and control of the quadrotor system. In the actual flight, for quadrotor flying at low altitude, it is more susceptible to wind field that could

Corresponding Author: Yanmin Chen, School of Transportation Science and Engineering, Beihang University, Beijing, 100191, China

significantly affect the aerodynamic performance and stability (Su *et al*., 2007). Therefore, it is necessary to take the impact of wind field into account in the study of quadrotor system's modeling and control.

To overcome this problem, in this study, a dynamic model of the quadrotor considering the influence of wind field is established. The quadrotor system is divided into two interconnected subsystem: rotor subsystem and body subsystem. The rotor subsystem's aerodynamic model which takes the impact of the wind field into consideration is built through blade element theory and momentum theory. The dynamic model of the body subsystem is established by Newton-Euler formalism. In order to control the position and attitude of the nonlinear system, an integral backstepping controller is designed and the system stability is conducted through the Lyapunov theory. Three numerical simulation experiments are demonstrated and the conclusions are drawn finally.

DYNAMIC MODEL OF QUADROTOR HELICOPTER SYSTEM

The quadrotor system is composed by body and four rotors, as presented in Fig. 1. Set up two reference frames: the earth-fixed reference frame $E = \{E_x, E_y, E_z\}$ and the body-fixed reference frame $B = \{B_x, B_y, B_z\}$. The absolute position $X = [x, y, z]^T$ and attitude angle $\Theta = [\varphi, \theta, \psi]^T$ of the system are defined in the reference frame *E*. These three Euler Angels are called roll angle $(-\pi/2<\varphi<-\pi/2)$, pitch angle $(-\pi/2<\theta<\pi/2)$ and yaw angle $(-\pi<\psi<\pi)$.
The rotation transformation matrix from ***B*** to ***E*** is:

$$\boldsymbol{R(\Omega)} = \begin{bmatrix} C_\psi C_\theta & C_\psi S_\theta S_\varphi - S_\psi C_\varphi & C_\psi S_\theta C_\varphi + S_\psi S_\varphi \\ S_\psi C_\theta & S_\psi S_\theta S_\varphi + C_\psi C_\varphi & S_\psi S_\theta C_\varphi - C_\psi S_\varphi \\ -S_\theta & C_\theta S_\varphi & C_\theta C_\varphi \end{bmatrix} \quad (1)$$

where, $S(.) = \sin(.)$ and $C(\cdot) = \cos(\cdot)$.

The thrust forces F_{Ti} (i =1, 2, 3, 4) is generated by the four rotors. The motion of the quadrotor is controlled by varying the rotation speed of the four rotors to change the thrust and the torque produced by each one. Four rotors are divided into two pairs-pair (1, 3) and pair (2, 4). The rotate direction of the two pairs is contrary in order to counteract the aerodynamic torque generated by the rotors' rotation. Increase or decrease the rotation speed of the four rotors simultaneously will generate vertical motion. Independently varying the speed of the rotor pair (1, 3) can control the pitch angle (θ) about the y-axis and the translational motion along the x-axis. Accordingly, independently varying the speed of the rotor pair (2, 4) can control the roll angle (φ) about the x-axis and the translational motion along the y-axis. The yaw angle (ψ) about the z-axis is determined by the yaw torque which is the sum of the reaction torques generated by each rotor.

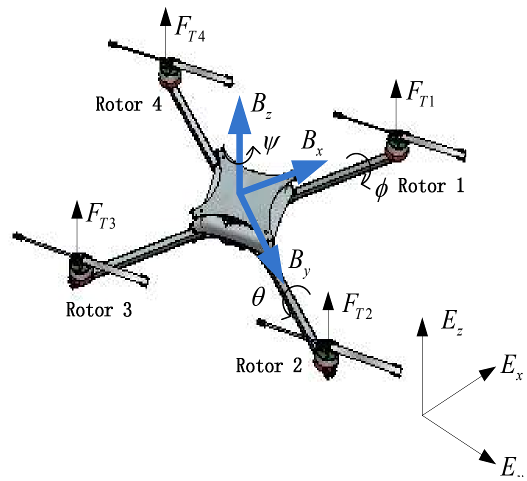

Fig. 1: Sketch of quadrotor helicopter

Rotor aerodynamics: The two speed coefficients advance ratio (μ) and inflow ratio (λ) of the rotor is:

$$\mu = \frac{U^B{}_x}{\Omega r} = \frac{V^B{}_x - R^T(\Omega)\cdot W^E{}_x}{\Omega r}$$
$$\lambda = \frac{v - U^B{}_z}{\Omega r} = \frac{v - (V^B{}_z - R^T(\Omega)\cdot W^E{}_z)}{\Omega r} \quad (2)$$

where, *U* is the air speed, *V* is the ground speed and *W* is the wind speed. In reference frame *G*, $W^E = [W^E{}_x, W^E{}_y, W^E{}_z]^T$ is a known quantity. Ω is the angular velocity of the rotor, *r* is the radius of the rotor, *v* is the induced velocity. The aerodynamic coefficients: thrust coefficient C_T, drag coefficient C_H, torque coefficient C_Q and roll coefficient C_R can be derived according to μ and λ, thereby the thrust force F_T, drag force F_H, torque M_Q and rolling moment M_R can be obtained:

$$\begin{bmatrix} \boldsymbol{F_T} \\ \boldsymbol{F_H} \\ \boldsymbol{M_Q} \\ \boldsymbol{M_R} \end{bmatrix} = \begin{bmatrix} C_T \rho A r^2 \boldsymbol{\Omega}^2 \\ C_H \rho A r^2 \boldsymbol{\Omega}^2 \\ C_Q \rho A r^2 \boldsymbol{\Omega}^2 r \\ C_R \rho A r^2 \boldsymbol{\Omega}^2 r \end{bmatrix} \quad (3)$$

where, $\rho = 1.293\ kg/m^3$ is the air density and *A* is the area of propeller disk.

System General Forces and Moments: Assume that the quadrotor is a rigid-body structure and is completely symmetrical. Establish the translational dynamic equation and the rotational dynamic equation according to Newton-Euler formalism.

Step 1: Establish the translational dynamic equation:

$$\boldsymbol{F_{total}} = m\ddot{\boldsymbol{X}} \tag{4}$$

where, F_{total} is the external resultant force, such as:

$$\boldsymbol{F_{total}} = \boldsymbol{F_{rotor}} - \boldsymbol{F_{aero}} - \boldsymbol{F_G} \tag{5}$$

where $F_G=mG$ is the gravity, $G = [0,0,g]^T$. F_{rotor} represents the aerodynamic forces of the rotor and F_{aero} is the air resistance of the body:

$$\begin{aligned} \boldsymbol{F_{rotor}} &= \boldsymbol{R(\Omega)}(\sum_{i=1}^{4}\boldsymbol{F_{Ti}} - \sum_{i=1}^{4}\boldsymbol{F_{Hi}}) \\ \boldsymbol{F_{aero}} &= \frac{1}{2}\rho A\boldsymbol{C}(\boldsymbol{U^B})^2 \end{aligned} \tag{6}$$

where, $\boldsymbol{C}=diag[C_x,C_y,C_z]$.

From Eq. (4-6), the translational dynamic equations are obtained:

$$\ddot{x} = \frac{1}{m}[(S_\varphi S_\psi + C_\psi S_\theta C_\varphi)\sum_{i=1}^{4}F_{Ti} - \sum_{i=1}^{4}F_{Hxi} - \frac{1}{2}\rho AC_x({U^B}_x)^2] \tag{7}$$

$$\ddot{y} = \frac{1}{m}[(-S_\varphi C_\psi + S_\psi S_\theta C_\varphi)\sum_{i=1}^{4}F_{Ti} - \sum_{i=1}^{4}F_{Hyi} - \frac{1}{2}\rho AC_y({U^B}_y)^2] \tag{8}$$

$$\ddot{z} = \frac{1}{m}(C_\theta C_\varphi\sum_{i=1}^{4}F_{Ti} - \frac{1}{2}\rho AC_z({U^B}_z)^2) - g \tag{9}$$

Step 2: Establish the rotational dynamic equation:

$$\boldsymbol{M_{total}} = \boldsymbol{I\ddot{\Theta}} + \boldsymbol{\dot{\Theta}} \times \boldsymbol{(I\dot{\Theta})} \tag{10}$$

where $\boldsymbol{M_{total}}$ is the external resultant moment, such as:

$$\boldsymbol{M_{total}} = \boldsymbol{M_c} + \boldsymbol{M_g} + \boldsymbol{M_R} \tag{11}$$

where, $\boldsymbol{M_g} = J_r \cdot (-1)^{i+1}\sum_{i=1}^{4}\boldsymbol{\dot{\Theta}} \times \boldsymbol{\Omega_i}$ is the gyroscopic torque of the rotor, J_r is the rotor's moment of inertia, $\boldsymbol{M_R} = (-1)^{i+1}\sum_{i=1}^{4}\boldsymbol{M_{Ri}}$ is the rolling moment and M_c is the control moment produced by the rotors:

$$\boldsymbol{M_c} = \begin{bmatrix} l(-\boldsymbol{F_{T2}} + \boldsymbol{F_{T4}}) \\ l(\boldsymbol{F_{T1}} - \boldsymbol{F_{T3}}) \\ (-1)^{i+1}\sum_{i=1}^{4}\boldsymbol{M_{Qi}} \end{bmatrix} \tag{12}$$

where, l is the arm length of the quadrotor. From Eq. (10-12), the rotational dynamic equations are obtained:

$$\ddot{\varphi} = \frac{I_{yy} - I_{zz}}{I_{xx}}\dot{\theta}\dot{\psi} - \frac{J_r}{I_{xx}}\dot{\theta}\Omega_r + \frac{1}{I_{xx}}(-1)^{i+1}\sum_{i=1}^{4}M_{Rxi} + \frac{l}{I_{xx}}(F_{T4} - F_{T2}) \tag{13}$$

$$\ddot{\theta} = \frac{I_{zz} - I_{xx}}{I_{yy}}\dot{\varphi}\dot{\psi} + \frac{J_r}{I_{yy}}\dot{\varphi}\Omega_r + \frac{1}{I_{yy}}(-1)^{i+1}\sum_{i=1}^{4}M_{Ryi} + \frac{l}{I_{yy}}(F_{T1} - F_{T3}) \tag{14}$$

$$\ddot{\psi} = \frac{I_{xx} - I_{yy}}{I_{zz}}\dot{\varphi}\dot{\theta} - \frac{J_r}{I_{zz}}\dot{\Omega}_r + \frac{1}{I_{zz}}(-1)^{i+1}\sum_{i=1}^{4}M_{Qi} \tag{15}$$

where, $\Omega_r = \Omega_1 - \Omega_2 + \Omega_3 - \Omega_4$.

INTEGRAL BACKSTEPPING CONTROL SCH EME

Integral backstepping control scheme is used for this system because:

- The backstepping technique is applicable to nonlinear system and has strong robustness to disturbances (Kanellakopoulos and Krein, 1993)
- The integral term of states parameters error is introduced to the backstepping technique in order to eliminate the static error of the system (Skjetne and Fossen, 2004)

Assume that the angular velocity of the system in reference frame E is equal to it in reference frame B; ignore the drag force, rolling moment of rotor and air resistance of body. Consider the thrust coefficient b and drag coefficient d as constants. Based on the above assumptions, the equation of the system model in state-space is obtained: $\dot{\boldsymbol{S}} = f(\boldsymbol{S},\boldsymbol{U})$, where $\boldsymbol{S} = [x,\dot{x},y,\dot{y},z,\dot{z},\varphi,\dot{\varphi},\theta,\dot{\theta},\psi,\dot{\psi}]^T$ is the state vector and $U = [U_1, U_2, U_3, U_4]^T$ is the input vector. The inputs U_1, U_2, U_3 and U_4 are defined as:

$$\begin{bmatrix} U_1 \\ U_2 \\ U_3 \\ U_4 \end{bmatrix} = \begin{bmatrix} b(\Omega_1^2 + \Omega_2^2 + \Omega_3^2 + \Omega_4^2) \\ b(-\Omega_2^2 + \Omega_4^2) \\ b(\Omega_1^2 - \Omega_3^2) \\ d(\Omega_1^2 - \Omega_2^2 + \Omega_3^2 - \Omega_4^2) \end{bmatrix} \tag{16}$$

where, U_1 is designed for altitude control and U_2, U_3, U_4 is used for the control of the three attitude angles respectively. The control equation is written as:

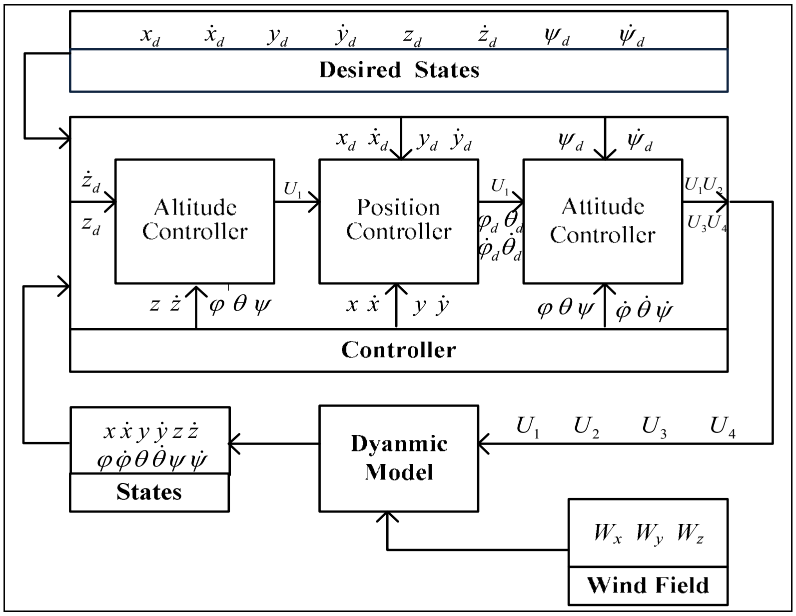

Fig. 2: Structure of control system

$$f(\boldsymbol{S},\boldsymbol{U}) = \begin{bmatrix} \dot{x} \\ \dfrac{C_\varphi S_\theta C_\psi + S_\varphi S_\psi}{m} U_1 \\ \dot{y} \\ \dfrac{C_\varphi S_\theta S_\psi - S_\varphi C_\psi}{m} U_1 \\ \dot{z} \\ \dfrac{C_\varphi C_\theta}{m} U_1 - g \\ \dot{\varphi} \\ \dot{\theta}\dot{\psi}\dfrac{I_{yy}-I_{zz}}{I_{xx}} + \dot{\theta}\dfrac{J_r}{I_{xx}}\Omega_r + \dfrac{l}{I_{xx}}U_2 \\ \dot{\theta} \\ \dot{\varphi}\dot{\psi}\dfrac{I_{zz}-I_{xx}}{I_{yy}} - \dot{\varphi}\dfrac{J_r}{I_{yy}}\Omega_r + \dfrac{l}{I_{yy}}U_3 \\ \dot{\psi} \\ \dot{\varphi}\dot{\psi}\dfrac{I_{xx}-I_{yy}}{I_{zz}} + \dfrac{l}{I_{zz}}U_4 \end{bmatrix} \tag{17}$$

The structure of the control system is shown in Fig. 2. The controller consists of three parts: attitude controller, altitude controller and position controller. Altitude controller outputs U_1 according to the desired altitude (z_d), current altitude (z) and attitude angle (φ,θ,ψ). Position controller receives U_1, combines the desired position (x_d,y_d) and current position (x,y), outputs desired roll angle (φ_d) and desired pitch angle (θ_d). Attitude controller receives desired attitude angle (φ_d, θ_d, ψ_d) and current attitude angle (φ,θ,ψ), outputs U_2, U_3, U_4. The dynamic model receives input vector from controller, integrates with wind field, outputs the state of next time step and feeds back to the controller.

Here we deduce the control of roll angle as an example to explain the design of controller.

Step 1: Set the tracking-error of roll angle (φ) as:

$$e_\varphi = \varphi_d - \varphi \tag{18}$$

Set the first Lyapunov function as:

$$V_1 = \frac{1}{2}(e_\varphi{}^2 + \lambda_1 \chi_1{}^2) \tag{19}$$

where, $\chi_1 = \int_0^t e_\varphi(\tau)d\tau$ is the integral of tracking-error of roll angle (φ), λ_1>0.
The derivation of Eq. (19) is:

$$\begin{aligned} \dot{V}_1 &= e_\varphi \dot{e}_\varphi + \lambda_1 \chi_1 e_\varphi \\ &= e_\varphi(\dot{e}_\varphi + \lambda_1 \chi_1) \\ &= e_\varphi(\dot{\varphi}_d - \dot{\varphi} + \lambda_1 \chi_1) \end{aligned} \tag{20}$$

If we set the virtual control $(\dot{\varphi})_d$ of $\dot{\varphi}$ as:

$$(\dot{\varphi})_d = \dot{\varphi}_d + \lambda_1 \chi_1 + c_1 e_\varphi,\ c_1 > 0 \tag{21}$$

then:

$$V_1 = -c_1 e_\varphi{}^2 \tag{22}$$

Hence when $e_\varphi \neq 0$, $\dot{V}_1 < 0$.
Set the tracking-error of $\dot{\varphi}$ as:

$$e_{\dot{\varphi}} = (\dot{\varphi})_d - \dot{\varphi} \quad (23)$$

Set the second Lyapunov function as:

$$V_2 = \frac{1}{2}(e_\varphi^2 + \lambda_1\chi_1^2 + e_{\dot{\varphi}}^2 + \lambda_2\chi_2^2) \quad (24)$$

where, $\chi_2 = \int_0^t e_{\dot{\varphi}}(\tau)d\tau$ is the integral of tracking-error of roll angular velocity ($\dot{\varphi}$), λ_2>0.
The derivation of Eq. (24) is:

$$\dot{V}_2 = e_\varphi((1+\lambda_1 - c_1^2)e_\varphi + \ddot{\varphi}_d + c_1 e_{\dot{\varphi}} - c_1\lambda_1\chi_1 - \ddot{\varphi} + \lambda_2\chi_2) - c_1 e_\varphi^2 \quad (25)$$

If we set the virtual control $(\ddot{\varphi})_d$ of $\ddot{\varphi}$ as:

$$(\ddot{\varphi})_d = (1+\lambda_1 - c_1^2)e_\varphi + \ddot{\varphi}_d + (c_1 + c_2)e_{\dot{\varphi}} - c_1\lambda_1\chi_1 + \lambda_2\chi_2 \quad (26)$$

where, c_1>0, c_2>0, then:

$$\dot{V}_2 = -(c_1 e_\varphi^{\ 2} + c_2 e_{\dot{\varphi}}^{\ 2}) \quad (27)$$

Hence when $e_\varphi \neq 0$ and $e_{\dot{\varphi}} \neq 0, \dot{V}_2 < 0$. We can know that the closed-loop system is asymptotically stable according to Lyapunov theorem.

Step 3: According to the control equation of roll angle (φ) in Eq. (17):

$$\ddot{\varphi} = \dot{\theta}\dot{\psi}(I_{yy} - I_{zz} / I_{xx}) + \dot{\theta}\Omega_r J_r / I_{xx} + U_2 l / I_{xx}$$

U_2 is obtained:

$$U_2 = \frac{I_{xx}}{l}[(1+\lambda_1 - c_1^2)e_\varphi + \ddot{\varphi}_d + (c_1 + c_2)e_{\dot{\varphi}} - c_1\lambda_1\chi_1 + \lambda_2\chi_2 - \dot{\theta}\dot{\psi}(I_{yy} - I_{zz}) / I_{xx} - \dot{\theta}\Omega_r J_r / I_{xx}] \quad (28)$$

Similarly, pitch angle (θ) control U_3 can be obtained:

$$U_3 = \frac{I_{yy}}{l}[(1+\lambda_3 - c_3^2)e_\theta + \ddot{\theta}_d + (c_3 + c_4)e_{\dot{\theta}} - c_3\lambda_3\chi_3 + \lambda_4\chi_4 - \dot{\varphi}\dot{\psi}(I_{zz} - I_{xx}) / I_{yy} + \dot{\varphi}\Omega_r J_r / I_{yy}] \quad (29)$$

where, $c_3, c_4, \lambda_3, \lambda_4$ are positive constants and χ_3, χ_4 are the integral of tracking-error of pitch angle (θ) and pitch angular velocity ($\dot{\theta}$).

Table 1: Structural parameters

Parameter	Definition	Value	Unit
m	Mass	0.723	kg
l	Arm length	0.314	m
J_r	Rotor inertia	7.321×10^{-5}	$kg \cdot m^2$
I_{xx}	X Inertia	8.678×10^{-3}	$kg \cdot m^2$
I_{yy}	Y Inertia	8.678×10^{-3}	$kg \cdot m^2$
I_{zz}	Z Inertia	3.217×10^{-2}	$kg \cdot m^2$
b	Trust factor	5.324×10^{-5}	$N \cdot s^2$
d	Drag factor	8.721×10^{-7}	$Nm \cdot s^2$

Table 2: Control parameters

Item	Value	Item	Value	Item	Value
c_1	10	c_2	3	c_3	10.5
c_4	3.5	c_5	4	c_6	3
c_7	4	c_8	2.5	c_9	3
c_{10}	1	c_{11}	2	c_{12}	1
λ_1~λ_{12}	0.05				

Yaw angle (ψ) control U_4 can be obtained:

$$U_4 = \frac{I_{zz}}{l}[(1+\lambda_5 - c_5^2)e_\psi + \ddot{\psi}_d + (c_5 + c_6)e_{\dot{\psi}} - c_5\lambda_5\chi_5 + \lambda_6\chi_6 - \dot{\varphi}\dot{\theta}(I_{xx} - I_{yy}) / I_{zz}] \quad (30)$$

where, $c_5, c_6, \lambda_5, \lambda_6$ are positive constants and χ_5, χ_6 are the integral of tracking-error of yaw angle (ψ) and yaw angular velocity ($\dot{\psi}$).
Altitude control U_1 can be obtained:

$$U_1 = \frac{m}{C_\varphi C_\theta}[g + (1 - c_7^{\ 2} + \lambda_7)e_z + (c_7 + c_8)e_{\dot{z}} - c_7\lambda_7\chi_7] \quad (31)$$

where, c_7, c_8, λ_7 are positive constants and χ_7 is the integral of tracking-error of altitude z.

SIMULATION RESULTS

This section validates the effective of proposed model and control scheme by three numerical simulation experiments. Firstly, we test the performance of the system in the absence of wind field. Then, wind field with velocity of $W^E = [1, 2, 0]^T$ m/s and $W^E = [3, 3, 0]^T$ m/s is introduced separately. Table 1 summarizes the structural parameters of the model. Table 2 lists the control parameters of the controller.

In the absence of wind field: Expect system hovering at $X = 1_{3\times1}$ m. The initial conditions is $X = 1_{3\times1}$ m, $\Theta = 0_{3\times1}$ rad, the desired conditions is $X_d = 1_{3\times1}$ m, $\psi_d = 0$ rad. The translational and rotational velocity in both initial and desired conditions is 0. The position and attitude angle response of the system in the absence of wind field are shown in Fig. 3 and 4. We can observe

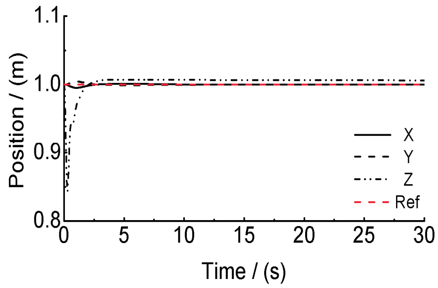

Fig. 3: Position response (in the absence of wind field)

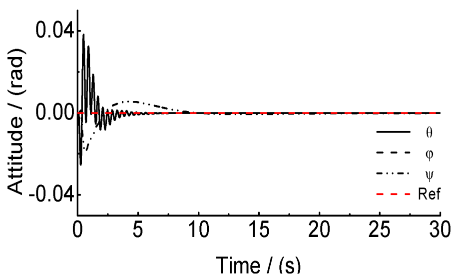

Fig. 4: Attitude angle response (in the absence of wind field)

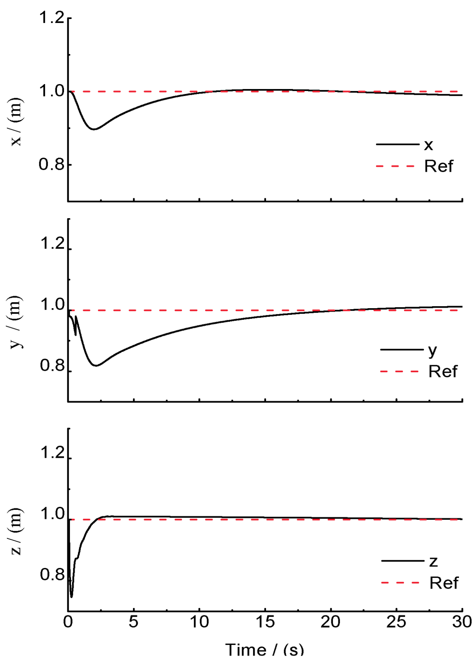

Fig. 5: Position response (In the presence of a $\boldsymbol{W_E} = [1, 2, 0]^T$ m/s wind field)

that the position reach to desired value rapidly; the attitude angle have slight oscillation at beginning, but the controller stabilized it at 0 rad in a short period of time. In this situation, the controller presents good performance.

In the presence of a $W^E = [1, 2, 0]^T$ m/s wind field: Maintain the same initial and desired conditions, the system's position and attitude angle response in the presence of a $W^E = [1, 2, 0]^T$ m/s wind field are shown in Fig. 5 and 6. We can see that the position can be stabilized at the desired value in about 15 seconds. Pitch angle (θ) is stabilized at 0.13 rad, roll angle (φ) is stabilized at -0.27 rad, This is due to the influence of lateral wind field, the aircraft nose of the two directions need to be placed into a certain angle in order to achieve hovering. For the wind speed in y direction is greater than it in x direction, the roll angle (φ) is larger than pitch angle (θ). In this situation, the oscillation of

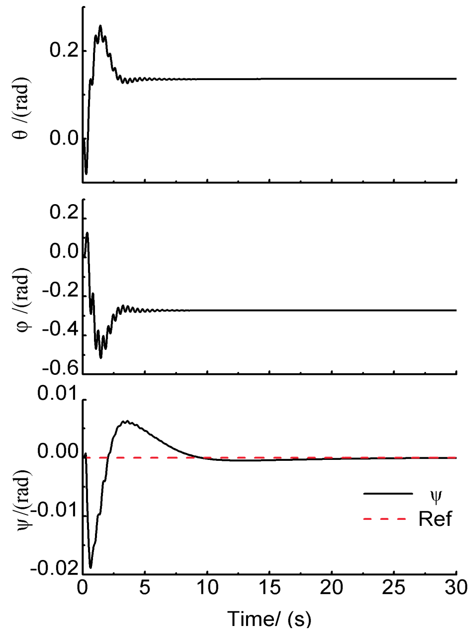

Fig. 6: Attitude angle response (In the presence of a $\boldsymbol{W_E} = [1, 2, 0]^T$ m/s wind field)

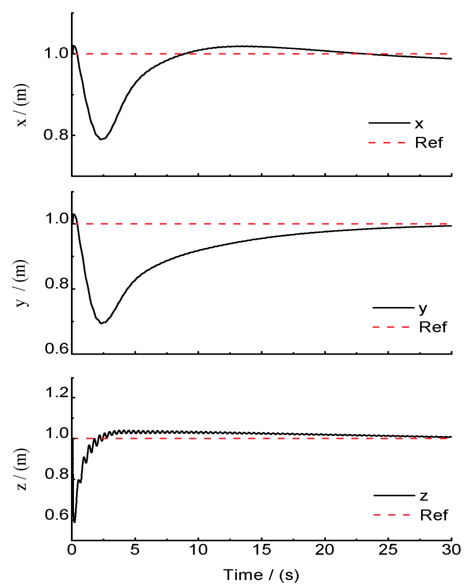

Fig. 7: Position response (in the presence of a $\boldsymbol{W_E} = [3, 3, 0]^T$ m/s wind field)

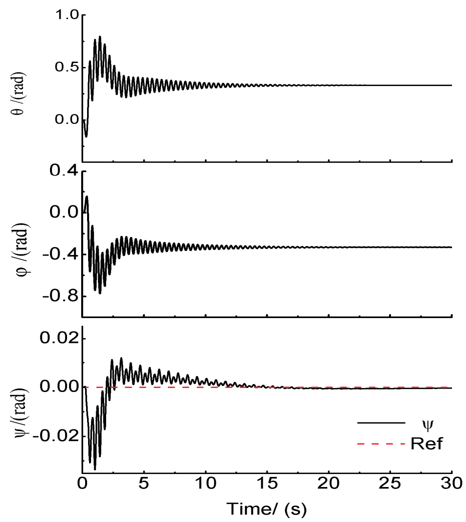

Fig. 8: Attitude angle response (In the presence of a W_E = [3, 3, 0]^T m/s wind field)

attitude angle and the time achieve stable are greater than them in experiment 1.

In the presence of a W^E = [3, 3, 0]^T m/s wind field: The wind speed is increased to W^E = [3,3,0]^T m/s, still maintaining the same initial and desired conditions, the system's position and attitude angle response in this experiment are shown in Fig. 7 and 8. We can observe that position can be stabilized at the desired value in about 20 seconds. Pitch angle (θ) is stabilized at 0.33 rad, roll angle (φ) is stabilized at -0.33 rad and both of them are larger than that in experiment 2. This is due to the increase of wind speed the aircraft nose needs to be placed into a lager angle in order to resists the reinforced wind. We can note that because the wind speed is equal in x direction and y direction in this experiment, pitch angle (θ) and roll angle (φ) are of the same. Compared with experiment 2, we can see that with the increase of wind speed, the oscillation of attitude angle and the time achieving stable are become greater.

CONCLUSION

The dynamic model of a quadrotor helicopter system under impact of wind field is established and the nonlinear controller based on integral backstepping algorithm is designed. The performance of the system under effect of wind field is studied by numerical simulation experiment. The conclusions from the results can be summarized as follows:

- Position and attitude angle response of the system is accurate to wind field and that is line with principles of flight dynamics; stable time and oscillation are greater when the speed of wind field is increased, this indicates the impact wind field reduce the stability of the system. Therefore, this model can accurately reflect the dynamic performance of the system in the effect of wind field
- The controller can make the system achieve hovering in the desired location even under the interference of wind field. Therefore, the controller has good performance.

ACKNOWLEDGMENT

This study is supported by the National Aerospace Science Foundation of China (2011ZA51).

REFERENCES

Abhijit, D., F. Lewis and K. Subbarao, 2009. Backstepping approach for controlling a quadrotor using Lagrange form dynamics. J. Intell. Robot. Syst., 56(12): 127-151.

Ashfaq, A.M. and D.B. Wang, 2008. Modeling and backstepping-based nonlinear control strategy for a 6 DOF quadrotor helicopter. Chinese J. Aeronaut., 21(4): 261-268.

Bouabdallah, S. and R. Siegwart, 2007. Full control of a quadrotor. Proceeding of IEEE/RSJ International Conference on Intelligent Robots and Systems. San Diego, CA, Oct 29-Nov 2, pp: 153-158.

Bouabdallah, S., A. Noth and R. Siegwart, 2004. PID vs LQ control techniques applied to an indoor micro quadrotor. Proceedings of the IEEE/RSJ International Conference on Intelligent Robots and Systems. Sendai, Japan, pp: 2451-2456.

Bouchoucha, M., S. Seghour and M.B. Osmani, 2011. Integral backstepping for attitude tracking of a quadrotor system. Electron. Electr. Eng., 116(10): 75-80.

Carrillo, L., E. Rondon and A. Sanchez, 2011. Stabilization and trajectory tracking of a quadrotor using vision. J. Intell. Robot. Syst., 61(14): 103-118.

Hoffmann, G.M., H. Huang and S. Waslander, 2011. Precision flight control for a multi-vehicle quadrotor helicopter test bed. Control Eng. Pract., 19(3): 1023-1036.

Hoffmann, G.M., S.L. Waslander and M.P. Vitus, 2009. Stanford testbed of autonomous rotorcraft for multi-agent control. Proceeding of IEEE/RSJ International Conference on Intelligent Robots and Systems. St. Louis, USA, October 11-15, pp: 404-405.

Kanellakopoulos, I. and P.T. Krein, 1993. Integral-action nonlinear control of induction motors. Proceedings of the 12th IFAC World Congress. Sydney, Australia, pp: 251-254.

Lee, D., H. Kim and S. Sastry, 2009. Feedback linearization vs. adaptive sliding mode control for a quadrotor helicopter. Int. J. Control Autom., 7(3): 419-428.

Madani, T. and A. Benallegue, 2006a. Backstepping sliding mode control applied to a miniature quad rotor flying robot. Proceeding of 32nd Annual Conference on IEEE Industrial Electronics. Paris, France, pp: 700-705.

Madani, T. and A. Benallegue, 2006b. Backstepping control for a quadrotor helicopter. Proceeding of IEEE/RSJ International Conference on Intelligent Robots and Systems. Beijing, China, October 11-15, pp: 3255-3260.

Raffo, G., M. Ortega and F. Rubio, 2010. An Integral predictive nonlinear H (Infinity) control structure for a quadrotor helicopter. Automatica, 46(1): 29-39.

Salih, A.L., M. Moghavvemi and H.A.F. Mohamed, 2010. Flight PID controller design for a UAV quadrotor. Proceeding of IEEE International Conference on Automation, Quality and Testing, Robotics. Cluj-Napoca, Romania, May 28-30, pp: 3660-3667.

Skjetne, R. and T.I. Fossen, 2004. On Integral control in backstepping: Analysis of different techniques. Proceedings of the 2004 American Control Conference. Boston, MA, USA, June 30-July 2, pp: 1899-1904.

Su, Y., Y. Cao and K. Yuan, 2007. Helicopter stability and control in the presence of wind shear. Aircr. Eng. Aerosp. Tec., 79(2): 170-176.